Proceedings of the 28th IEEE
EMBS Annual International Conference
New York City, USA, Aug 30-Sept 3, 2006

A multi-modal 2D/3D registration scheme for preterm brain images

Jef Vandemeulebroucke, Ewout Vansteenkiste, Wilfried Philips

Abstract— **Periventricular Leukomalacia (PVL) is a neonatal brain pathology occuring on preterms with a very low birth weight (< 1500g). Next to ultrasound (US) imaging, which is the first and most common step, Magnetic Resonance Image (MRI) volumes are used for the inspection of this pathology. Since on both modalities, up to now, we still lack a golden standard for the quantification of the pathology cross-validation through a multi-modal registration is highly beneficial to the clinical diagnosis. In this article we present a semi-automatic 2D US - 3D MRI registration scheme combining an interactive initialization step, B-spline image interpolation, a mutual information based metric and an evolutionary algorithm optimization scheme.**

I. Introduction

1.2 % of the newborns are Very Low Birth Weight (VLBW) infants ($\leq$ 1500g). The recent increase in survival rate of these VLBW infants has brought along an increasing incidence of neurological sequelae [1]. Here we will focus on one particular brain pathology, called Periventricular Leukomalacia (PVL), which in its milder variant is characterized by deep white matter lesions adjacent to the lateral ventricles, also called flaring, see Fig. 1. This is the primary indication of further abnormal brain development. Among the survivors of the neonatal period, 50 % is normal at the age of 6, 10-20 % suffer from severe handicaps.

In previous work [1], [2] PVL has already been studied on MRI volumes as well on newborns as on the outcome on later stages. Other work [3], [4] already showed the possibility of detecting PVL based on US images. The non-invasiveness and portability of the US machine make this modality highly suitable given the nature of the patients. On the other hand, due to the speckle noise present, the visual inspection of the images is often subjective.

Although MRI volumes are less noisy, they are harder to capture when dealing with non-sedated preterms. Next to that, we still lack a golden standard for the quantification of the flaring both in US as well as in MRI. Therefore, physicians nowadays believe valuable information can be obtained from the simultaneous inspection of the US and the corresponding MR image. In order to obtain this objective image comparison, the images should contain exactly the same anatomical features and thus have to be registered correctly.

In literature, many 3D/3D registration algorithms have been presented for different modalities, also including US. The 2D/3D case is often less trivial given there is less information available for the same number of degrees of freedom. Next to that, 2D/3D schemes are commonly found for CT, PET, MRI modalities, but the typical speckle noise in the US images makes it hard to create this kind of registration scheme, although there is a clear demand for it. Here we will try to fill the gap by presenting an interactive registration scheme, to our knowledge the first on neonatal US brain imaging.

In the next sections, we will first explain the data used, Section II, then present our registration scheme, Section III, show some experimental results in Section IV, before presenting our conclusions in Section V.

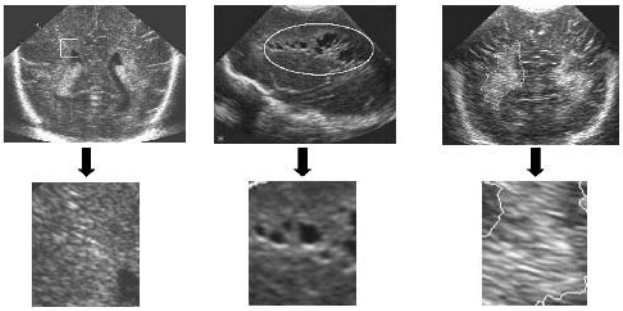

Fig. 1. On the left a normal brain and part of the periventricular zone below it. In the middle, a cystyc PVL brain and below it a clear cut-out of the cysts in the tissue that come with the severe variant of the pathology. On the right, the gliotic PVL with the flaring delineated and below a cut-out of the periventricular flaring.

II. Data Acquisition and Preprocessing

A total of 20 coronal 2D-US brain images obtained from 20 preterms up to 32 weeks of gestation were analyzed. All images were captured in the first 3 weeks after birth at the Sophia Children's hospital Rotterdam, The Netherlands, by one medical expert using an Acuson Sequoia 512 ultrasound machine with a hand-free 8.5 MHz probe. The US image pixel size is 0.16×0.16 mm. Consequently, 20 MRI volumes of the same patients were acquired using a General Electric 1.5T Sigma Infinity scanner. A T1 weighted volume containing about 85 images at a voxel size of $0.85 \times 0.85 \times 1$ mm and T2 weighted volume containing about 20 images at a voxel size of $0.70 \times 0.70 \times 4$ mm were used in the registration process. The acquisition time for the MRI images lay between 4 and 5 minutes. Given an US scan angle of about 45 degrees to the coronal plane, the MRI sequences were rotated over the same angle in order to obtain a better initialization.

Jef Vandemeulebroucke is with Universidade Federal de Santa Catarina, Departamento de Automao e Sistemas, Florianpolis, Santa Catarina, CEP 88040-900, Brasil jef@das.ufcr.br

Ewout Vansteenkiste and Wilfried Philips are with Faculty of Telecommunication and Information Processing, Image Processing and Interpretation Group, Ghent University, Sint-Pietersnieuwstraat 41, 9000 Ghent, Belgium ervsteen@telin.ugent.be

III. Registration scheme

A. Mechanism

Fig. 2 illustrates our registration scheme, apart from the previously explained initialization steps. We will briefly discuss this scheme before going into detail on the most important parts. First, we have to decide on which image will be fixed in a space coordinate system, and which one will be transformed resulting each time in a new overlap. We choose thee 2D-US image as fixed, the MRI volume as

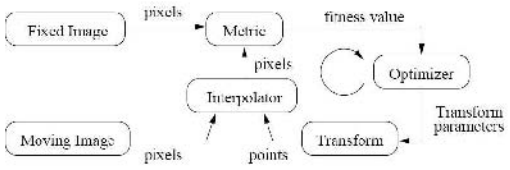

Fig. 2. Schematic overview of the registration.

moving. For each possible overlap, an interpolator calculates the values of the moving image at the grid positions of the fixed image. On this overlap, we calculate a metric value, which is an adequate indicator for the similarity between the current overlapping (MR) slice and the fixed (US) image. Based on this metric value, an optimizer then proposes new transform parameters. Before we can evaluate this new candidate solution, the interpolator once again finds the intensities of the moving image at the grid positions of the fixed image. This cycle is repeated until the optimal transform is found or a stopping criterium is reached.
In technical terms, suppose u is our reference image and v our test volume, and $u(x)$ and $v(x)$ are the corresponding pixels or voxels. Denote by T a transformation of the coordinate system of the reference image to that of the test volume and by F_c a function that reaches a maximum when the registration is correct. Then the registration goal is to find the optimal estimate transformation T_c, so that

$$T_c = arg \max_T F_c(u(x), v(T(x))). \quad (1)$$

B. Transform

Since we include 3D volumes, we consider 6 degrees of freedom, allowing translations and rotations around the three principal axes. The head is considered a rigid object so scaling is not applied. The transform is centered, meaning the center of rotation can be chosen arbitrary other than in an origin based implementation. A natural choice is the center of the head, which leads to an easier interpretation of and a reduced dependency on the transform parameters. If for example all parameters are set to their optimal values, varying one rotation angle will result in the volume rotating, while still remaining in an overlapping position with the US image. A similar movement with a not-centered transform would require changes in all 6 transform parameters. In Fig. 3, a 2-dimensional example is given, illustrating both types of transforms.

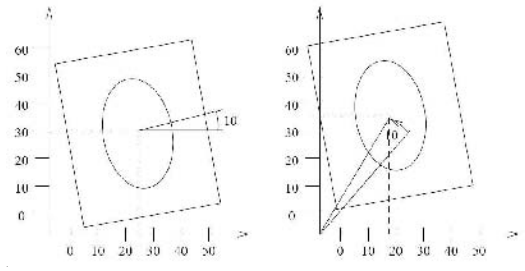

Fig. 3. on the left a rotation around a center, on the right a rotation around the origin.

C. Interpolator

The scan time for the MRI volumes has to be limited and we are restricted to work by the protocols put forward by the medical doctors. This implies a non-neglectable difference between the resolution of both modalities. For example, the US images used have a resolution of 0.16×0.16 mm while the T2 weighted MRI volume has a resolution of $0.7 \times 0.7 \times 4$ mm. Hence we interpolate the MRI volume, to assure acceptable registration results. As interpolating is computationally expensive, it is essential to use an time-efficient algorithm. For this reason a simple linear interpolation is performed in each iteration of the scheme.
For some volumes however, as the T2 weighted volume, it is necessary to perform a more complex interpolation before the actual registration procedure starts, since just applying a linear interpolation would result in images of poor quality. That is why the MRI volume is first upsampled using B-splines of degree 5. In order not to increase the memory usage exponentially, we created isotropic voxels of size 0.5mm in that way. Fig. 4, shows an example of an interpolation using B-splines.

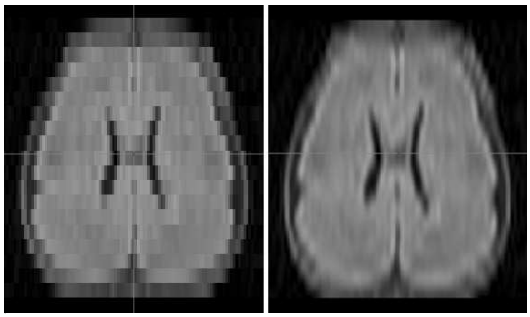

Fig. 4. on the left the original MR image (z-direction), on the right the B-spline interpolated MR image.

D. Metric

This component is undoubtedly the most critical. The metric value is the result of a mathematical measure, based on the values of the group of pixels relevant for the current solution and reflects the quality of this solution. Since we are working with different modalities, we can not just compare the intensities of corresponding pixels the two images.

Here we used an implementation of the Mutual Information algorithm provided by Mattes et al. [6] which is computationally more interesting than the one proposed by Viola et al. [5]. For more details we refer to the reference paper, but mainly only one sample set is used throughout the entire run of the program and B-splines, having a finite support, instead of Gaussian kernels are used in order to estimate the probability density functions (PDF). For the calculation of the entropy, no second sample set is needed but the estimated PDF's, uniformly distributed over the intensity interval, are evaluated. The advantage of this metric is that it uses only 2 parameters: the number of samples used to estimate the PDF, and the number of histogram bins used to calculate the entropy.

E. Optimizer

The optimizer finds the optimal transformation parameters. It searches the 6-dimensional space to efficiently zoom in on the optimal solution, while not getting caught in local extrema of the metric. A $(1+1)$-evolutionary strategy was implemented, which has proven to be more robust and effective in this kind of environment.

The strategy starts from a set op possible initial solution and combines them in a specific way as to obtain new generations of solutions. Suppose we obtain a solution x_t, at iteration t. A new solution x_{t+1} is then generated, satisfying:

$$x_{t+1} = x_t + a_t r_t$$

where r_t is a normally distributed random variable:

$$r_t \sim N(0,1)$$

and a_t satisfies:

$$a_t = \begin{cases} a_{t-1} c_{grow} & \text{if } F(x_t) > F(x_{t-1}) \\ a_{t-1} c_{shrink} & \text{else.} \end{cases}$$

Note that here we assume a higher value $F(x)$ corresponds to a better solution. The parameters a_0, x_t, c_{grow}, c_{shrink} are set priorly. Here, x_0 is an initialization of T, the value of c_{grow} en c_{shrink} are set according to [7], and are close to 1. The algorithm stops when a prefined maximum number of generations is reached or if a_t is smaller then a prefined threshold ε.

Intuitively, we impose normal variations on a solution at a certain stage scaled by a factor a_t. If we find a better solution than the current one we increase this factor, thus supposing even better solutions may lay even further away, improving the exploration of the search space. If no better solution is found we decrease this factor, thus supposing a better solution can be found through the exploitation of the local neighborhood. The small number of floating point operations makes the algorithm very fast and allows us to generate many generations without enlarging the computation time significantly. Another advantage of these optimizations is their relative insensitivity to local optima in the metric, allowing the technique to perform well in noisy environments, such as the US images.

The major drawback is that the solution is not always unique and so multiple runs have to be taken into account to base the final result on. As mentioned above the low computational complexity makes this possible.

	r_x	r_y	r_z	t_x	t_y	t_z
$P1_i$	-0.8	0	0	0	11.3	11.3
$P1_f$	-0.81	-0.0077	-0.0049	-0.340	10.6	11.8
$P2_i$	-0.8	0	0	0	-10	-10
$P2_f$	-0.79	0.0087	0.0011	-2.94	-7.5	-11.79
$P3_i$	-0.8	0	0	0	-13.2	-13.2
$P3_f$	-0.59	0.0054	0.025	1.23	12.065	-11.48
$P4_i$	-0.8	0	0	0	-16	-16
$P4_f$	-0.63	-0.034	-0.0505	2.71	-12.43	-16.80

TABLE I

FOR EACH OF THE 4 PATIENTS THE INITIAL (P_i) AS WELL AS FINAL (P_f) TRANSLATION/ROTATION PARAMETERS ARE SHOWN.

IV. EXPERIMENTAL RESULTS

Fig. 5 shows the visual results of the registration of 4 different patients. The mosaic images are shown as well as the corresponding US and MR image. The upper two image groups are based on T1 weighted volumes, the lower two on T2 weighted volumes. All results were obtained using the same protocol. First, the appropriate US region of interest was selected, then the MRI volumes were interpolated using the B-splines, rotated of a 45 degrees angle and an initial starting slide was chosen. As such transform was initialized as

$$T_i = (-0.8,\ 0,\ 0,\ 0,\ \frac{t_z}{\sqrt{2}},\ \frac{t_z}{\sqrt{2}})$$

with t_z the z-coordinate of the initial slide, first 3 coordinates presenting the rotation (in radials), last three the translation.

Instead of using an initial random solution for the evolutionary algorithm, a Regular Step Gradient Descent method combined with the Mattes mutual information was run on T_i, leading to the initial starting point for the scheme presented earlier. This was found more stable than any arbitrary selection. The registration procedure was then run 15 times and the optimal registration result was selected based on the results of the metric, next to the visual evaluation of the results. The optimal translation/rotation parameters for the two patients can be found in the Table.

Optimal results differed 0.1 mm in translation and 0.01 radials in rotation compared to the manual registration of a medical expert, which is very good given the very small size of the head. We should mention however that solely based on the results of the metric, the rotational variance might be bigger and not always we succeed in achieve the optimal result. Therefore, a visual inspection of the best outcomes is indeed necessary. Note also that the final results often are rather close to the initializations so a good initialization is very important.

When looking at the visual results, also see Fig. 6, we see the outer structures of the brain are usually registered well, there were for the inner parts it is less obvious. This can be explained by the fact that some features such as the Plexus Chorideus, an anatomical region inside of the

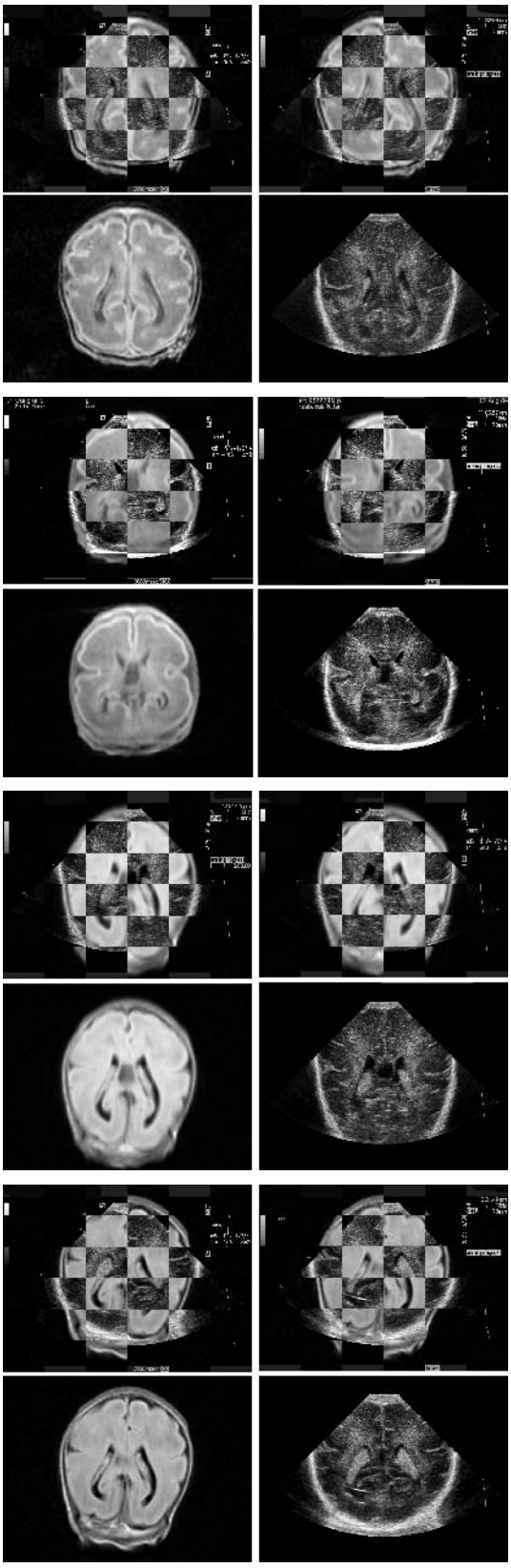

Fig. 5. Registration results for 4 different patients, the upper two T1 weighted images, the lower two a T2 weighted images.

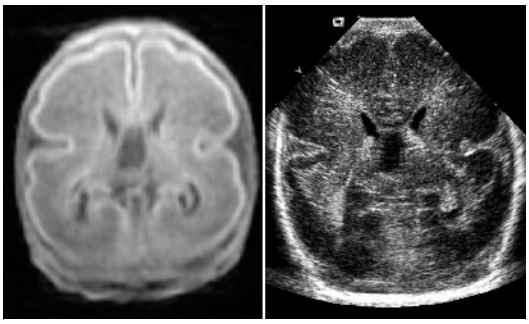

Fig. 6. Registered MR and US image. The Plexus Chorideus is the bright white spot at the bottom of each central ventricle. Notice is has, amongst other features, a different appearence on the MR and US image.

lateral ventricles, are displayed differently due the intrinsic properties of the different modalities. This makes the US registration very hard and calls for a visual interpretation of the results as mentioned above.

Finally no real difference was found in the registration results for the T1 and T2 weighted images, altough the T1 images tend to show more detailed information, making them more suitable for visual diagnosis.

V. Conclusions

We constructed a 2D US - 3D MRI registration method with limited user-interaction. The program automatically places both images in the space coordinate system, after upsampling the MRI volume. The user then roughly initializes the transform, after which an evolutionary strategy optimizes a mutual information based metric. Visual results, as shown in Fig. 5, are satisfying and have been validated by the clinical experts.

As a continuation of our work we would like to test how a feature-based metric could even further improve the registration process as well as possible speckle suppression as a preprocessing to the registration algorithm. Based on this registration, first steps are also taken in order to cross-validate the specific segmentation and classification results found on both modalities separately.

References

[1] D. Davis. Review of cerebral palsy. *Neonatal Network* ,16,7-12,1997.

[2] N. Paneth, R. Nudelli, E. Kazam and W. Monte. Brain Damage in the preterm infant. *Mac Keith Press*, London,1994.

[3] S. Fujimoto, N. Yamaguchi, H. Togari, Y. Wada and K. Yokochi. Cerebral palsy of cystic periventricular leukomalacia in low-birth-weight infants. *Acta Paediatr*,83,397-401,1994.

[4] F. Pidcock, L. Graziani, C. Stanley, D. Mitchell and D. Merton. Neurosonographic features of periventricular echodensities associated with cerebral palsy in the preterm infant. *Journal of Pediatrics*,116,417-422,1990.

[5] P. Viola and W. M. Wells III. Alignment by maximization of mutual information. *IJCV*,24(2):137154, 1997.

[6] D. Mattes, D. R. Haynor, H. Vesselle, T. K. Lewellen, and W. Eubank. Non-rigid multimodality image registration. *Medical Imaging 2001: Image Processing*, pages 1609-1620, 2001.

[7] M. Styner and G. Gerig. Parametric Estimation of 2D/3D Bias Correction with 1+1ES-Optimization. *Techmical Report*,Image Science Lab ETH Zürich,1997.